ARTICLES
PUBLISHED ONLINE: 20 MAY 2012 | DOI: 10.1038/NPHOTON.2012.108
nature photonics

An invisible metal–semiconductor photodetector

Pengyu Fan[1], Uday K. Chettiar[2], Linyou Cao[1†], Farzaneh Afshinmanesh[1], Nader Engheta[2] and Mark L. Brongersma[1*]

Nanotechnology has enabled the realization of hybrid devices and circuits in which nanoscale metal and semiconductor building blocks are woven together in a highly integrated fashion. In electronics, it is well known how the distinct material-dependent properties of metals and semiconductors can be combined to realize important functionalities, including transistors, memory and logic. We describe an optoelectronic device for which the geometrical properties of the constituent semiconductor and metallic nanostructures are tuned in conjunction with the materials properties to realize multiple functions in the same physical space. In particular, we demonstrate a photodetector in which the nanoscale electrical contacts have been designed to render the device 'invisible' over a broad frequency range. The structure belongs to a new class of devices that capitalize on the notion that nanostructures have a limited number of resonant, geometrically tunable optical modes whose hybridization and intermodal interference can be tailored in a myriad of useful ways.

In current electronic and photonic circuitry, metals and semiconductors serve different functions that can be traced to their distinct material-dependent properties. For example, metals have high electrical conductivities and are frequently used for charge transport, injection or extraction. Their high optical reflectivity allows mirrors and gratings to reflect or redirect light. Meanwhile, semiconductors have valuable electrical properties that can be controlled by doping, and they feature useful optical properties that enable light generation, detection or modulation. Traditional optoelectronic device design aims to maximize the performance of individual electronic and optical building blocks based on a specific materials property and then to assemble the pieces. This has resulted in the development of systems in which the electronic and optical functions are spatially separated and easily recognized.

Here, we describe a photodetector that belongs to a new class of chip-scale devices that not only exploit the unique material-dependent properties of semiconductors and metals, but also capitalize on the notion that nanostructures of these materials exhibit strong and tunable optical responses that critically depend on their geometry and size[1]. The realization of such a device requires a new design methodology in which the geometrical properties of the constituent building blocks have to be carefully tuned in conjunction with their material properties. As the electronic side of such optimizations is well understood, we focus on a discussion of the optical optimization. First, subwavelength building blocks are chosen based on their desired electrical and optical material properties. Second, the limited number of optical resonances of the building blocks is identified as well as their tunability with size, shape and dielectric environment. Third, the building blocks are assembled in a subwavelength region and one or more desired optical functions are realized by capitalizing on strong modal hybridization and intermodal interference effects between these small objects. This procedure typically has a number of constraints that are determined by the electronic requirements (for example, electrical connectivity). In this delicate harmonization process, the optimization of specific geometries and sizes in fact becomes as important as the materials selection. In the resulting device, the constituent semiconductors and metals naturally play an electronic (charge extraction) and optical (cloaking) function at the same time and in the same physical space. Moreover, the traditional spatial boundaries between electronic and photonic components have disappeared and new opportunities for ultradense integration emerge.

Figure 1a presents a schematic of the proposed photodetector, in which the metallic contacts overcoat a semiconductor nanowire. Its design started with a materials selection based on the desired electrical and optical properties. We chose a silicon nanowire for its excellent electronic transport properties and its ability to transduce light to photocurrent. We chose to place a high-electrical-conductivity metal (gold) contact on top of the wire to enable efficient charge extraction. From an optical perspective, it is not intuitively clear whether coating the nanowire with a reflective metal would be beneficial. However, we will show that the geometrical properties of the metallic contacts and the semiconductor nanowire can be re-engineered to perform several valuable optical functions, including the first experimental demonstration of a cloaking sensor in the visible part of the electromagnetic spectrum.

In the second design step, we considered the optical modes of the metal contact and the high-refractive-index silicon nanowires. The optical properties of metal nanostructures are by now quite well established. These negative-dielectric-constant (ε) objects support surface plasmon (SP) resonances, which are collective oscillations of free electrons that couple to electromagnetic fields[1]. Recently, a wide range of useful optical functions have been realized by shaping and arranging resonant nanometallic structures. Among the promising applications are nanoscale optical waveguides[2], nanometallic antennas[3], metamaterials exhibiting a negative index[4,5] or intriguing polarization properties[6], and new types of cluster matter that exhibit magnetic and Fano-like resonances[7] or structural induced transparency[8,9]. The latter two effects have been used successfully to significantly suppress light scattering at a target frequency of operation, and the present work makes use of the basic concepts that underlie these intriguing phenomena to render an optoelectronic device invisible. To build a device, it is

[1]Geballe Laboratory for Advanced Materials, Stanford University, California 94305, USA, [2]Department of Electrical and Systems Engineering, University of Pennsylvania, Philadelphia, Pennsylvania 19104, USA; [†]Present address: Department of Materials Science and Engineering, North Carolina State University, Raleigh, North Carolina 27695, USA. *e-mail: brongersma@stanford.edu

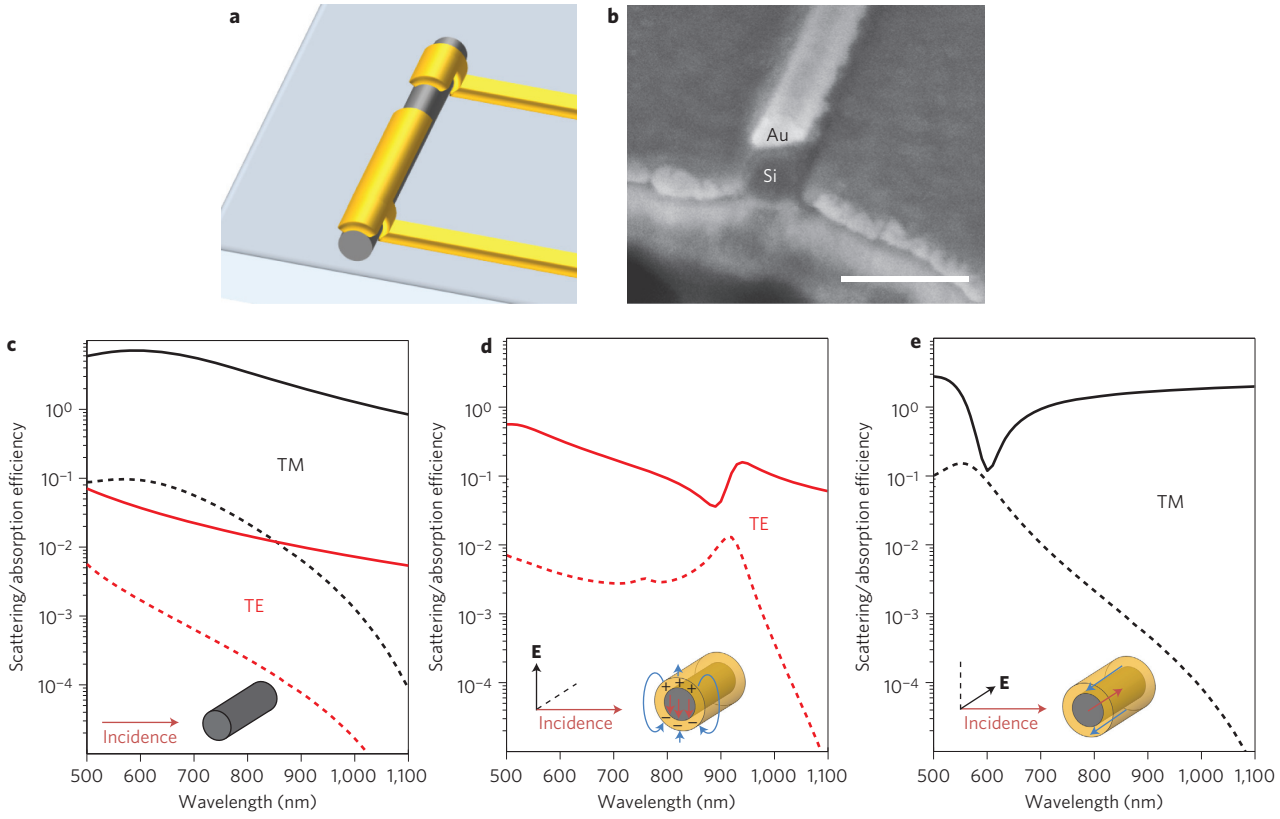

Figure 1 | Design and operation of a hybrid gold/silicon nanowire photodetector. a, Schematic of a silicon nanowire (grey) hooked up by two gold electrodes (yellow). **b**, SEM image of a 50-nm-diameter silicon nanowire with a 20-nm-thick gold 'cover'. Scale bar, 100 nm. **c**, Scattering (solid curves) and absorption (dashed curves) cross-sections as a function of wavelength for a 50-nm-diameter silicon nanowire. Scattering and absorption are much stronger under TM illumination (black curves) than under TE illumination (red curves) due to the presence of a strong optical TM resonance near 600 nm. **d**, Scattering and absorption cross-sections for the same silicon nanowire as in **c**, but with a 15-nm-thick gold shell under TE illumination. For TE illumination, scattering and absorption are greatly enhanced in the hybrid structure. The peak around 900 nm in the silicon absorption is attributed to a dipolar SP resonance. **e**, For TM illumination, the silicon core and gold shell are polarized in opposite directions, and this gives rise to a dramatic reduction in the scattering efficiency of the hybrid structure; in practical terms, the wire becomes invisible or 'cloaked' near 600 nm.

essential to introduce semiconductors, and to hide it from the eye we need both the metal and semiconductor components to exhibit optical resonances. It has already been convincingly shown that optical coupling of plasmonic structures with semiconductor nanostructures that support excitonic excitations is opening up a new field of quantum plexcitonics[10]. Here, we use a strongly geometry-dependent optical resonance that naturally occurs in high-dielectric-constant semiconductor nanostructures. These resonances are associated with the excitation of leaky optical modes of the nanostructure and are distinct from resonant optical excitations of an electronic transition[11,12]. Interestingly, they can occur in deep-subwavelength structures (~10 nm) as small as state-of-the-art electronic components. For example, the semiconductor nanowires used in the proposed detector show tunable light scattering and absorption resonances that rival the strength of plasmonic resonances[13]. They have been used in applications including films with vibrant structural colours[14], solar cells[15] and ultrafast photodetectors[16]. In such structures, the resonances result from the ease with which large displacement currents are driven inside a semiconductor nanostructure. Here, we aim to join geometrically resonant metallic and semiconductor nanostructures together into highly functional hybrid devices that derive their properties from their near-field coupling and intermodal interference. It is important to note that the resonances of both metallic and semiconductor nanostructures are broadband and are typically associated with leaky modes that enable effective optical antenna functions. For this reason, these structures can find application in broadband, chip-scale nanodevices that naturally interface with the outside world and as building blocks for transmissive metamaterials.

Figure 1b shows a cross-sectional scanning electron microscopy (SEM) image of our proposed hybrid nanowire photodetector consisting of a 50-nm-diameter silicon nanowire with a 20-nm-thick gold cover. Spectral light scattering and photocurrent experiments on this type of structure are described in the following, and the fabrication is detailed in the Methods. In the third design step, we explore how the optical response of the hybrid semiconductor/metal structure can be tailored by engineering the interaction between the modes of the silicon nanowire and gold contact. The possible interactions are first examined in two idealized model systems: a bare silicon nanowire and a silicon nanowire with a concentric gold shell (Fig. 1c–e, insets). The optical response of these structures is strongly polarization-dependent. For top-illuminated cylinders, the optical modes can be divided into transverse-magnetic (TM, with the electric field along the axis of the nanowire) and transverse-electric (TE, with the electric field normal to the axis of the nanowire) modes. The scattering and absorption efficiencies of the different wires were calculated as a function of wavelength for both polarizations using Mie theory[17,18]. In these preliminary calculations, shown in Fig. 1c–e, only light absorption inside the silicon wire is included as its magnitude determines the number of photocarriers that could be extracted from a nanowire detector. Figure 1c shows the scattering (solid curves) and absorption (dashed curves) efficiencies of the bare silicon nanowire for TM

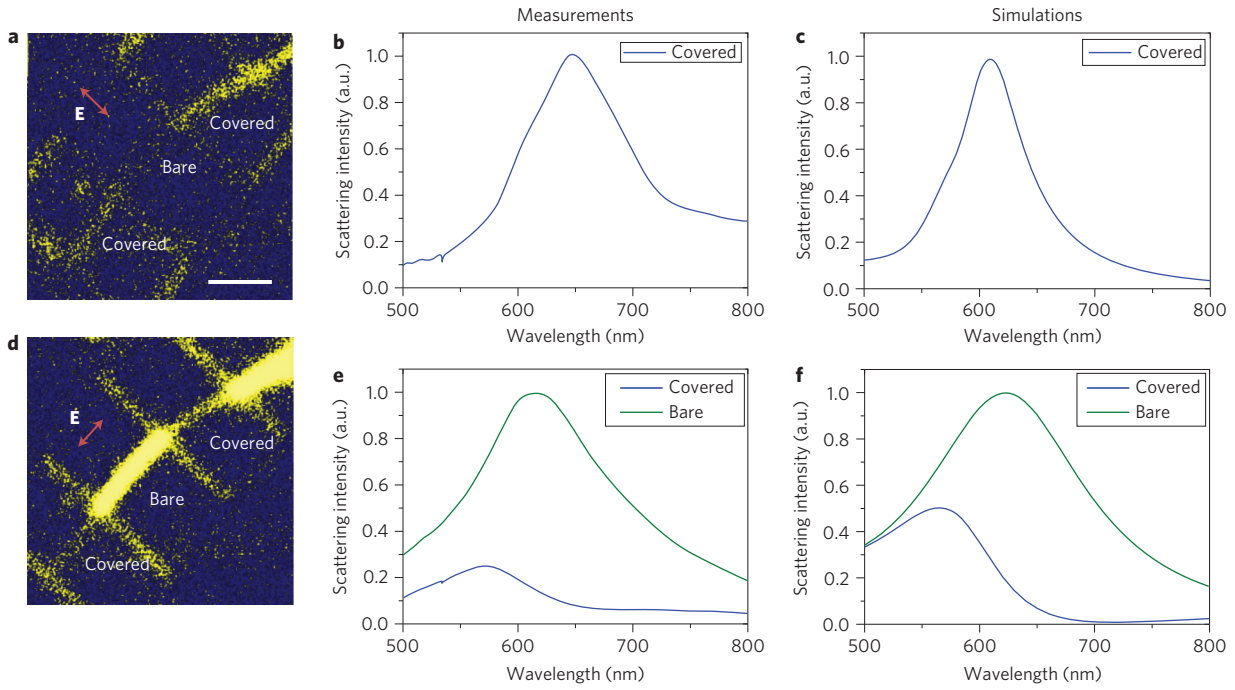

Figure 2 | Polarization-dependent light-scattering phenomena for a gold-covered silicon nanowire. a,**d**, Images of a 50 nm silicon nanowire captured confocally under TE (**a**, first row) and TM (**d**, second row) illumination with white light (scale bar, 2 μm). The bare and gold-covered regions of the wire are indicated in the images. **b**,**e**, Experimentally determined scattering spectra for the bare and covered regions for TE (**b**) and TM (**e**) illumination. A plasmonic resonance is clearly observed under TE illumination (**b**) and the cloaking effect of the gold cover is seen under TM illumination (**e**). **c**,**f**, Simulated scattering spectra corresponding to the experimental spectra in **b** and **e**, respectively.

(black) and TE (red) illumination. The spectral region of interest from 500 nm to 1,100 nm shows a strong lowest-order, monopolar TM_{01} resonance in the scattering and absorption that peaks near 620 nm. The subscripts refers to the azimuthal mode number ($m = 0$), which indicates an effective number of wavelengths around the wire circumference, and the radial order number ($l = 1$), which describes the number of radial field maxima within the cylinder. Physically, the excitation of this mode corresponds to a displacement current that is driven back and forth along the wire axis with a maximum in the core of the wire. Under TE illumination, both the scattering and absorption are much weaker and exhibit a monotonic decay with increasing wavelength. This is explained by the absence of TE resonances in this spectral region. For both polarizations, light scattering form the nanowire dominates the absorption inside the semiconductor. This is a direct consequence of the relatively weak materials absorption of indirect-gap, crystalline silicon in this wavelength range.

Figure 1d,e shows that the addition of a gold shell dramatically alters the optical response of the silicon nanowire for both TE and TM illumination. The inset to Fig. 1d shows how a particle-like SP resonance can be driven in the gold shell under TE illumination[19]. The excitation of SPs produces high fields inside the silicon wire. As such, the shell effectively serves as an optical antenna capable of concentrating light into the wire and enhancing the photoresponse. A significant plasmonic enhancement in the photoresponse is seen at a wavelength near 900 nm and, owing to a dipolar resonance in the gold shell, both the scattering by the hybrid wire and the absorption inside the silicon peak around this wavelength. Figure 1e shows that the scattering efficiency under TM illumination is of a similar magnitude as that of the bare nanowire near 500 nm and 1,100 nm. However, near 600 nm, a two orders of magnitude reduction in the scattering efficiency is observed. This effect is explained by realizing that under TM illumination both the wire and gold cover are strongly polarized along the wire axis. In this example, the shell thickness was carefully chosen such that incident light at 600 nm induces an electric dipole moment in the shell that is equal in magnitude but opposite in sign to the dipole moment in the wire. This results in a net-zero total electric dipole moment in the combined wire/shell system. The deep-subwavelength size of the hybrid wire cross-section ensures that the opposing dipoles cancel one another's scattering in the far-field. This phenomenon is known as plasmonic cloaking[20]. Although the net dipole moment of the coated wire is zero, the dipole moment in the silicon wire can be large and this implies that photocarriers are generated. Such a cloaked sensor was in general terms speculated upon by Alù and Engheta[21]. As predicted, the absorption and radiation losses in this hybrid system result in the relatively broadband response.

We next describe the optical properties of the fabricated silicon nanowire detectors with a non-concentric gold cover (Fig. 1b). Light-scattering measurements on this structure were performed with a confocal optical microscope (see Methods). Figure 2a shows a confocal image of a 50-nm-diameter silicon wire on a gold substrate that is overcoated with a 20 nm gold cover in two rectangular regions. The image was taken with TE-polarized white light. In the gold-coated regions, the silicon wire is significantly brighter than in the uncoated regions. This is expected, because for this polarization, SPs are excited in the gold cover and cause strong light scattering. The bare wire is virtually imperceptible against the background due to the weak scattering under TE illumination[11]. To confirm the importance of a SP resonance in enhancing the visibility of the wire in the metal-coated region, a scattering spectrum was taken from the wire in the metal-coated area (Fig. 2b). The spectrum shows one strong peak in the red part of the spectrum. Its spectral features are in good qualitative agreement with the SP-induced scattering resonance seen in simulations (Fig. 2c). The difference in peak wavelength is attributed to the high sensitivity of the resonance position to both the dimensions

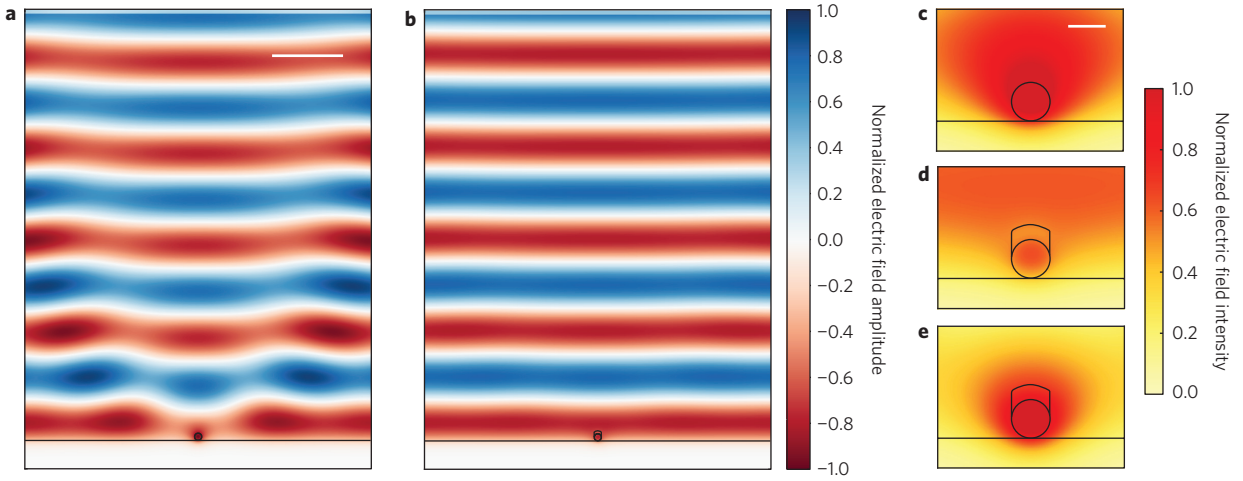

Figure 3 | Comparison of the electric field distribution surrounding a bare and a cloaked nanowire on a gold substrate under TM incidence. A snap shot (in time) of the real part of the electric field amplitude distribution (see colour bar on the right). Scale bar, 500 nm. **a**, Light scattering from a bare 50-nm-diameter silicon wire distorts the regular interference pattern produced by the incoming and reflected waves from the planar gold substrate. **b**, At the cloaking wavelength of 650 nm, the placement of a thin gold cover on top of the wire restores the planar wavefronts and the wire effectively become invisible. **c**–**e**, Comparison of the distribution of electric field intensity inside a bare silicon nanowire at 650 nm (**c**), a cloaked gold-covered silicon nanowire at the same wavelength (**d**), and the same gold-covered wire as in **d**, but for a shorter illumination wavelength of 580 nm (**e**), away from the cloaking condition. Scale bar in **c** is 50 nm.

and exact shape of the gold cover. This sensitivity is illustrated in the Supplementary Information (for example, Supplementary Fig. S6) and highlights the need for nanometre-scale control over the geometric parameters of the device.

Figure 2d presents a confocal image of the same region taken under TM-polarized white-light illumination. Compared to Fig. 2a, this image shows a contrast reversal between the metal-coated and bare nanowire regions with the gold-covered regions appearing much dimmer than the bare wire segments. This is in agreement with the predicted cancellation in the scattering due to plasmonic cloaking shown in Fig. 1e. To confirm this point, experimental and simulated scattering spectra were obtained from the bare and covered wire regions (Fig. 2e,f). In both cases, the gold cover produces a significant drop in the scattering intensity over a broad wavelength range in the visible spectrum, and the nanowire essentially becomes 'invisible'. A blueshift in the peak position from ~620 nm to 580 nm is also observed in both sets of spectra, in agreement with the blueshift seen in our model system (dashed black lines in Fig. 1c,e). This blueshift is also directly observable in colour images taken for the different nanowire sections (see Supplementary Information). The addition of the gold cover results in a stronger spatial confinement of the mode inside the silicon wire, pushing the resonance towards shorter wavelengths.

Full-wave simulations can help visualize the cloaking effect of a gold cover placed on the silicon nanowire. Figure 3a,b shows the electric field distribution for a TM-illuminated silicon nanowire on a gold substrate with (Fig. 3b) and without (Fig. 3a) a gold cover. The simulation was performed at a wavelength of 650 nm. Light scattering from the bare wire distorts the regular interference pattern produced by the incoming and reflecting waves from the planar gold substrate. The placement of the gold cover restores the planar wavefronts and the wire effectively become invisible. This is explained by the dramatically reduced scattering of the hybrid gold/silicon wire system near the cloaking wavelength. It is important to realize that the observed cloaking is quite insensitive to the illumination angle and the exact shape and placement of the metal and semiconductor regions (see Supplementary Information and ref. 22). The key requirement is to obtain a net-zero total electric dipole moment from the oppositely polarized semiconductor and metal regions. This mainly sets the requirements on the relative fractions of metal and semiconductor. For this reason, both the model system with a concentric gold shell and our real wire with a partial gold cover exhibit cloaking. This also explains why the use of lossy materials such as gold and silicon do not prevent cloaking.

It is worth exploring how the performance of a cloaked nanowire photodetector is affected by the presence of the gold cloak. Intuitively, one might expect that the presence of a reflective and lossy metal could significantly reduce light absorption and thus the photocarrier generation rate in the wire. Figure 3c,d shows the electric field intensity distribution in the bare and gold-cloaked silicon nanowires for TM illumination at a wavelength of 650 nm. Light absorption in the silicon nanowire is directly related to the electric field intensity in the wire. In the bare silicon nanowire the field is high due to the excitation of a strong TM_{01} resonance, as described above. The gold-covered wire exhibits a peak in intensity inside the wire that is reduced by a mere factor of 1.8, and the maximum field intensity inside the wire is still twice as large as the incident field. It is clear that the gold cover does not preclude light from entering the wire, in contrast to transformation-optics-based cloaking techniques, which aim to exclude fields from the cloaked region[4,23–25]. In fact, at wavelengths where the cloaking condition is not met, field intensities can be reached that are equal in magnitude to those seen in the bare wire. This is shown in Fig. 3e, which presents the field distribution in the gold-cloaked silicon nanowire at a shorter wavelength of 580 nm. It is clear that the gold-covered wire can still absorb light efficiently due to the excitation of a weakly perturbed TM_{01} resonance, which characteristically features the maximum field intensity in the centre of the semiconductor wire. It can be concluded that the presence of the gold cover does not preclude the use of a gold-covered wire as a high-performance detector, even at the wavelength where it is invisible. This is particularly true as resonant nanowires can significantly outperform planar structures in terms of the light absorption per unit volume (by a factor of >20)[16].

Photodetectors utilizing gold-covered silicon nanowires were experimentally tested in the configuration shown in Fig. 1a,b and as discussed in more detail in the Methods. Figure 4a shows the

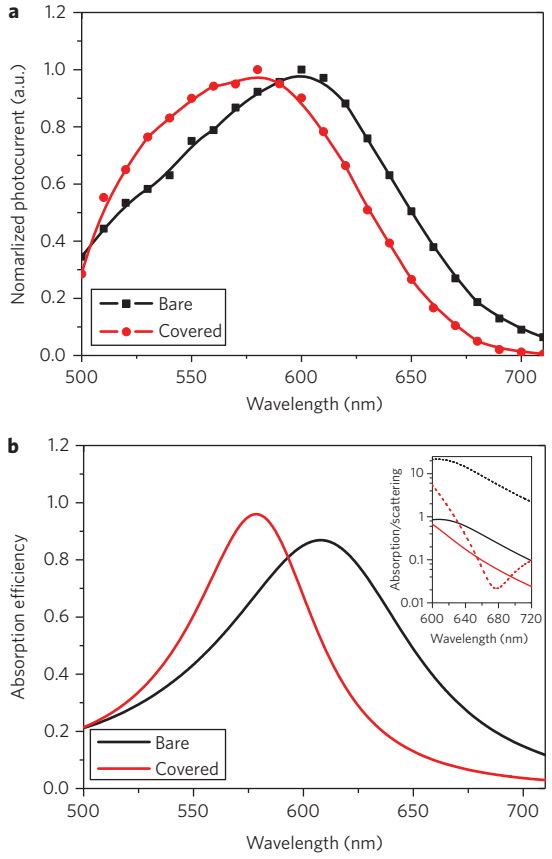

Figure 4 | Spectral absorption properties of bare and gold-coated silicon nanowires. a, Spectral photocurrent measurement (normalized) taken under TM illumination for a bare 50 nm silicon nanowire device (black) and for the same device after deposition of a 20-nm-thick gold cover on the wire (red). **b**, Simulations of the spectral absorption efficiency for the bare (black curves) and gold-covered (red curves) nanowire. Experiments and simulations both show a blueshift of the spectra for the covered wire. Inset to **b**: side-by-side comparison of scattering (dashed curves) and absorption (solid curves) for the bare (black curves) and covered (red curves) nanowire around 670 nm (plotted on a logarithmic scale). The gold cover causes a dramatic decrease in scattering, as shown by the valley on the red dashed curve, but the variation of absorption as a function of wavelength is much smoother.

measured photocurrent spectra taken from 50-nm-diameter silicon nanowire photodetectors with and without the gold cover for TM polarization (with the electric field vector parallel to the nanowire axis) where plasmonic cloaking is observed. To highlight the spectral changes that result from the gold cover, the photocurrent spectra for the gold-coated and bare silicon nanowires were normalized to the peak value. The bare wire exhibits strong light absorption (and thus photocurrent generation) due to the excitation of a TM_{01} resonance just above 600 nm. The peak in the photocurrent is close to the scattering resonance shown in Fig. 2d. The gold cover shifts the photocurrent (that is, absorption) and scattering resonances to the blue by several tens of nanometres. These trends are reproduced in the simulations of scattering (Fig. 2f) and absorption (Fig. 4b) efficiencies. The simulations also confirm that the absorption in the wire is decreased by a factor of just four, whereas the scattering from the wire is dramatically reduced by over two orders of magnitude due to cloaking (Fig. 4b, inset). According to these results, the ratio of the absorption and scattering efficiencies of a partially gold-covered nanowire can be enhanced by a factor of 80 and, under the idealized conditions illustrated in Fig.1, this ratio could reach a value of 2,400 at the cloaking wavelength.

Many relevant technologies, including solar cells, sensors, solid-state lighting, thermal photovoltaics and radiation management, chip-scale lasers and imaging technologies combine semiconductors and metals on a subwavelength scale. It is expected that the geometry of some of the structures currently in use could be reengineered so that the constituent materials can simultaneously perform valuable electronic (for example, charge injection or application of electric fields) and optical functions (for example, cloaking and optical antenna functions). As nanotechnology has spurred the development of increasingly complex metallic and semiconductor nanostructures, many new opportunities are emerging for combining these elementary photonic building blocks in hybrid devices that manipulate and actively control the flow of light at the nanoscale.

Methods

Silicon nanowire arrays were grown with an average diameter of 50 nm using a gold-catalysed chemical vapour deposition process[26]. The wires were first dispersed onto a gold-coated silica substrate, then a 20 nm gold layer was deposited via electron beam evaporation to create a thin gold cover on the nanowires, as shown schematically in Fig. 1a and in the cross-sectional SEM image in Fig. 1b.

Scattering and absorption efficiency calculations for idealized cylindrically symmetric silicon/gold core–shell nanowires were carried out analytically using the Mie–Lorentz formalism as described in ref. 17 and as defined in the Supplementary Information. For the real experimental structures, the scattering and absorption spectra and spatial field distribution were numerically obtained using a finite-difference time-domain technique. All simulations adopted the experimental, tabulated permittivity functions for both gold and silicon that include loss.

To investigate experimentally the optical properties of gold-coated silicon nanowires, light-scattering measurements were carried out on single nanowires using a confocal optical microscope (Nikon) coupled to a charge-coupled device camera and spectrometer. Using a Nikon ×100 dark-field objective, the nanowires were illuminated under grazing incidence with polarized white light and the light scattered upwards was collected.

For the detectors, ~200-nm-thick metallic contacts were patterned by electron-beam lithography and lift-off to produce devices as illustrated in Fig. 1a. Spectral photocurrent measurements were carried out with a white-light supercontinuum source (Fianium) coupled to an acousto-optical tunable filter (Fianium). To obtain high signal-to-noise ratio measurements, the illumination source was chopped and the photocurrent signal was measured using a source meter (Keithley) coupled to a lock-in amplifier (Stanford Research Systems). More details about the current–voltage characteristics of our detectors are presented in the Supplementary Information.

Received 26 January 2012; accepted 11 April 2012; published online 20 May 2012

References

1. Schuller, J. A. *et al.* Plasmonics for extreme light concentration and manipulation. *Nature Mater.* **9,** 193–204 (2010).
2. Brongersma, M. L., Hartman, J. W. & Atwater, H. A. Electromagnetic energy transfer and switching in nanoparticle chain arrays below the diffraction limit. *Phys. Rev. B* **62,** 16356–16359 (2000).
3. Novotny, L. Effective wavelength scaling for optical antennas. *Phys. Rev. Lett.* **98,** 266802 (2007).
4. Pendry, J. B., Schurig, D. & Smith, D. R. Controlling electromagnetic fields. *Science* **312,** 1780–1782 (2006).
5. Shalaev, V. M. Optical negative-index metamaterials. *Nature Photon.* **1,** 41–48 (2007).
6. Klein, M. W., Enkrich, C., Wegener, M. & Linden, S. Second-harmonic generation from magnetic metamaterials. *Science* **313,** 502–504 (2006).
7. Fan, J. A. *et al.* Self-assembled plasmonic nanoparticle clusters. *Science* **328,** 1135–1138 (2010).
8. Kekatpure, R. D., Barnard, E. S., Cai, W. & Brongersma, M. L. Phase-coupled plasmon-induced transparency. *Phys. Rev. Lett.* **104,** 243902 (2010).
9. Liu, N. *et al.* Plasmonic analogue of electromagnetically induced transparency at the Drude damping limit. *Nature Mater.* **8,** 758–762 (2009).
10. Manjavacas, A., Abajo, F. J. G. a. d. & Nordlander, P. Quantum plexcitonics: strongly interacting plasmons and excitons. *Nano Lett.* **11,** 2318–2323 (2011).
11. Cao, L. Y. *et al.* Engineering light absorption in semiconductor nanowire devices. *Nature Mater.* **8,** 643–647 (2009).
12. Schuller, J. A., Taubner, T. & Brongersma, M. L. Optical antenna thermal emitters. *Nature Photon.* **3,** 658–661 (2009).
13. Muskens, O. L. *et al.* Large photonic strength of highly tunable resonant nanowire materials. *Nano Lett.* **9,** 930–934 (2009).
14. Cao, L. Y., Fan, P. Y., Barnard, E. S., Brown, A. M. & Brongersma, M. L. Tuning the color of silicon nanostructures. *Nano Lett.* **10,** 2649–2654 (2010).

15. Cao, L. Y. *et al*. Semiconductor nanowire optical antenna solar absorbers. *Nano Lett.* **10,** 439–445 (2010).
16. Cao, L. Y., Park, J. S., Fan, P. Y., Clemens, B. & Brongersma, M. L. Resonant germanium nanoantenna photodetectors. *Nano Lett.* **10,** 1229–1233 (2010).
17. Mie, G. Articles on the optical characteristics of turbid tubes, especially colloidal metal solutions. *Ann. Phys. Berlin* **25,** 377–445 (1908).
18. Bohren, C. F. & Huffman, D. R. *Absorption and Scattering of Light by Small Particles* (Wiley, 1983).
19. Kreibig, U. & Vollmer, M. *Optical Properties of Metal Clusters* (Springer, 1995).
20. Alù, A. & Engheta, N. Achieving transparency with plasmonic and metamaterial coatings. *Phys. Rev. E* **72,** 016623 (2005).
21. Alù, A. & Engheta, N. Cloaking a sensor. *Phys. Rev. Lett.* **102,** 233901 (2009).
22. Silveirinha, M. G., Alù, A. & Engheta, N. Cloaking mechanism with antiphase plasmonic satellites. *Phys. Rev. B* **78,** 205109 (2008).
23. Cai, W. S., Chettiar, U. K., Kildishev, A. V. & Shalaev, V. M. Optical cloaking with metamaterials. *Nature Photon.* **1,** 224–227 (2007).
24. Valentine, J., Li, J., Zentgraf, T., Bartal, G. & Zhang, X. An optical cloak made of dielectrics. *Nature Mater.* **8,** 568–571 (2009).
25. Leonhardt, U. Optical conformal mapping. *Science* **312,** 1777–1780 (2006).
26. Cui, Y., Lauhon, L. J., Gudiksen, M. S., Wang, J. F. & Lieber, C. M. Diameter-controlled synthesis of single-crystal silicon nanowires. *Appl. Phys. Lett.* **78,** 2214–2216 (2001).

Acknowledgements

The authors acknowledge support from a Multidisciplinary University Research Initiative grant (Air Force Office of Scientific Research, grant no. FA9550-10-1-0264), the Air Force Office of Scientific Research (AFOSR; grant no. FA9550-08-1-0220) and the Interconnect Focus Center, one of six research centres funded under the Focus Center Research Program (FCRP), a Semiconductor Research Corporation entity. P.F. would also like to acknowledge support from Stanford Graduate Fellowship.

Author contributions

P.F., N.E. and M.L.B. conceived the experiments. P.F. and U.K.C. performed numerical simulations. L.C. performed silicon nanowire growth. P.F. performed sample fabrication and carried out all measurements. F.A. assisted with photocurrent measurement. P.F. and M.L.B. wrote the first draft of the manuscript. All authors discussed the results and contributed to the final version of the manuscript.

Additional information

The authors declare no competing financial interests. Supplementary information accompanies this paper at www.nature.com/naturephotonics. Reprints and permission information is available online at http://www.nature.com/reprints. Correspondence and requests for materials should be addressed to M.L.B.